Voltage Responsive Distribution Networks: Comparing Autonomous and Centralized Solutions

Paul Cuffe, *Member IEEE*, Andrew Keane, *Senior Member IEEE*

***Abstract*—Power system voltage control has traditionally been the responsibility of transmission-connected reactive power resources. Accordingly, high penetration levels of distributed generation present new challenges for reactive power management. Simply stipulating voltage control operation for distributed generators will not generally deliver voltage-responsive reactive power flows at the transmission system level, due mainly to the voltage-isolating effects of tap-changing bulk supply transformers. Additionally, the resistance of distribution system conductors establishes an unhelpful interaction between active power flows and voltage magnitudes. This work uses optimal power flow techniques to explore two ways to overcome these challenges. Most innovatively, a methodology is presented to optimally select static voltage control settings for distributed generators and transformers, such that they will provide an autonomous voltage-responsive behaviour without supervisory control systems. In this scheme, distributed generators are exposed to transmission voltage fluctuations as far as is feasible, by blocking the tapping of the bulk supply transformer when operating within an optimally-determined range of transmission voltages. Comparatively, an active control scheme is presented, where reactive power and tap positions are dispatched period-to-period to support the transmission system voltage. Comparing these approaches suggests the level of smart-grids investment required to effectively harness the reactive power available from distributed generation.**

***Index Terms*—distributed generation, voltage control, optimal power flow, active network control, autonomous control**

I. Introduction

The increase of renewable generation on certain power systems has seen a greater portion of the generation portfolio connected to the distribution system [1]. This shift may make the provision of ancillary services problematic for the transmission system operator [2,3]. This work speaks to the pressing topic of steady-state reactive power provision from distributed generators [1,4] in a highly renewable power system, addressing one of the problems reported in the case study of [5]. Modern renewable generators may offer a controllable reactive power resource [6]. Failure to harness such resources may materially increase the cost of renewables facilitation [7-9] as, fundamentally, any power system must maintain a regional reactive power balance, which may be problematic under renewables-driven displacement of synchronous plant [10].

This paper seeks a new, synergistic mode of interaction between the distribution and transmission systems. Can distributed reactive power resources respond helpfully to transmission system voltage fluctuations? Notably, simply enabling local voltage control for distributed generators will not generally deliver a desirable reactive power response at the transmission level. This work considers two approaches to delivering the desired behaviour: a novel autonomous control scheme, which doesn't require smart grid infrastructure, as well as a centrally controlled scheme, which does.

In the autonomous control scheme, each generator operates independently [11,12] with its own optimally-selected static controller settings, with no need for supervisory systems. This approach builds on previous work by the authors; [13,14] quantified how voltage-controlling distributed generators can deliver reactive power to the transmission system, a capability demonstrated to be tangibly useful for system-wide voltage security in [7,15]; [16] shows how optimally-selected static power factor settings for distributed generators can substantially reduce draw-down of reactive power from the transmission network. This last reference concludes that enhanced static power factor settings can offer performance comparable to that available with a full smart grid scheme.

The present work asks a similar question: can enhanced static voltage control settings deliver useful reactive power performance, or can this only be provided by active control schemes? Under the local control scheme, an optimal power flow tool is used to select enhanced static voltage control settings as well as parameters for an unusual use of transformer tap-blocking; under the smart control scheme, the reactive power output of generators is dispatched directly in every period, as are transformers' tap positions.

The optimal power flow framework that underpins both the control schemes is described in Section II. A test system is presented in Section III. The results of the optimization methodologies are presented in Section IV, with a load flow validation of the derived settings given in Section V. Conclusions on the comparative merits of each control approach are presented in Section VI.

II. Optimization Methodologies

For various reasons, it is not simple to make reactive power flows from distributed generators responsive to transmission-level voltages. Firstly, tap-changing action at the bulk supply transformer isolates distributed generators from higher-level voltage fluctuations, impeding a natural reactive power response. Secondly, active power exports tend to create

This work was conducted in the Electricity Research Centre, University College Dublin, Ireland, which is supported by the Commission for Energy Regulation, Bord Gáis Energy, Bord na Móna Energy, Cylon Controls, EirGrid, Electric Ireland, EPRI, ESB International, ESB Networks, Gaelectric, Intel, SSE Renewables, UTRC and Viridian Power & Energy.

P. Cuffe (paul.cuffe@ucd.ie) was funded through the SFI Research Frontiers Programme under grant number 09/RFP/ECE2394. A. Keane is funded through the Science Foundation Ireland (SFI) Charles Parsons Energy Research Awards.

voltage rise at distributed generator connection points, which necessitates a corrective import of reactive power to maintain a consistent local voltage. This coupling between active and reactive power flows is unavoidable due to the non-negligible resistance of distribution system conductors. Thirdly, active power flows within the distribution network itself invoke reactive power consumption, affecting the reactive power deliverable at the transmission level.

These difficulties are here overcome under two separate control paradigms. Both methodologies draw on the ac optimal power flow tool first described in [17], in addition to previous enhancements given in [13] and [18]; taken together, these references elucidate the detailed model whose treatment here is somewhat abbreviated for brevity. Central to the tool are the power flow equations for π-equivalent medium length lines, supplemented by the essential bounding constraints on such variables as node voltages. The resulting system of equations can be searched to local optimality using non-linear programming techniques.

A. Optimal Power Flow for Autonomous Control

Various enhancements to the optimization tool have been implemented for the *autonomous* control aspect of the present work, most notably a unique objective function, the use of voltage controller settings as control variables, the optimal dimensioning of withstandable external voltage deviations, and the use of a multi scenario analytic perspective. The optimal power flow tool is applied to an intact distribution network, considered in separation from the broader power system.

1) Multi Scenario Analysis

To permit selection of optimal, invariant settings that will be suitable over the full range of intact network loadings, a multi-scenario optimization is implemented. The field of security-constrained optimal power flow (e.g [19,20]) offers guidance here, where multiple network topologies are simultaneously considered, ensuring the universal feasibility, and optimality, of any settings derived. The present scheme draws on the treatments of [16,21], where representative combinations of network loadings, generation levels, and, for the first time here, external voltage conditions, are given simultaneous consideration within the optimization, while topology remains fixed. Thus, a single invocation of the optimization tool will return multi scenario vectors, indexed by t, for each network variable. For the *autonomous* scheme, the control variables are necessarily fixed across all scenarios, as no central coordination of the network is in view. The feasibility of the enhanced settings for network scenarios not considered within the optimization cannot be assured, and so the connection of new generators or loads will require a new application of this optimization methodology.

2) Autonomous Objective Function

While optimal power flow techniques have traditionally been used in pursuit of readily apparent objectives such as the minimisation of losses [22], such applications do not exhaust its capabilities [23]. The present methodology employs a novel objective function which *maximizes* the aggregate reactive power response of the distribution network to voltage deviations arising at its interfacing transmission system bus. An objective function could be formulated in various ways to deliver this type of response: the precise implementation described here reflects substantial effort invested in tuning the most computationally tractable solution.

Each distribution network seeks to influence the voltage at its interface point with the transmission network, which is denoted $V_{tx,t.}$ The objective function maximizes the network's reactive power response in periods when this external voltage deviates from the desired setting, V_{thresh}. A coherent voltage response calls for an injection of reactive power into the transmission system when voltage there are under V_{thresh}, and this is denoted by positive values of the reactive power exchange variable, $q_{tx,t}$.

The desired autonomous response is given by simultaneously maximizing the aggregate reactive power *injection* across all under-voltage scenarios and the *absorption* for the over-voltage scenarios:

$$max \quad \sum_{t|V_{tx,t}<V_{thresh}} q_{tx,t} \quad , \quad \sum_{t|V_{tx,t}>V_{thresh}} -q_{tx,t} \qquad (1)$$

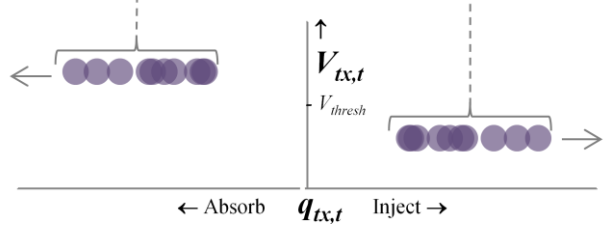

Fig. 1 A graphical illumination of the objective function, showing the desired relationship between V_{tx} and q_{tx}

The chosen objective function does not seek to perfectly replicate the behaviour of a transmission-connected voltage controller. The maximization of reactive power exchanges along the horizontal axis is denoted by the grey arrows in Fig. 1, as this behaviour is given *explicit* consideration in (1), whereas the vertical dimensioning is an *implicit* goal that naturally scales to facilitate the objective's maximization. The depiction of precisely two levels for $V_{tx,t}$ in Fig. 1 reflects modelling decisions described in the following sub-section.

3) Autonomous Static Control Variables

The control variables made available to the optimization tool for autonomous control are each generator's (g index) voltage control set-point, V_g^{set}, and voltage droop percentage, V_g^{droop}, as well as the static voltage ratio of the network's bulk supply transformer, T_{bsp}^{ratio}. This latter variable functions as a (continuous) proxy to the (discrete) optimal tap setting, and relates high and low-side voltages through the transformer lumped-impedance model. These variables, which remain invariant between scenarios, interact to establish voltage and reactive power relationships within the distribution network, with strong implications for the response maximized by (1).

A further control dimension is provided by introducing a new variable, S, which scales the voltage deviations imposed at the external node. This permits optimal specification of the maximum and minimum transmission system voltages, $V_{tx,t}$, which the network can withstand exposure to, in any loading

condition, while maintaining its static optimal tap setting (cf. [24] for a discussion of transformer tap blocking in a more conventional context). When the transmission-side voltage strays outside the range specified by *S*, conventional transformer voltage regulation must resume.

To facilitate the optimal selection of *S*, the external voltage for each scenario is specified by an input deviation term, $\Delta V_{tx,t}$, around the specified voltage threshold. The prevailing external voltage is then given by the following equality constraint:

$$V_{tx,t} = V_{thresh} + S\Delta V_{tx,t} \quad (2)$$

In this work, each load and generation combination is represented *twice* in the input scenario specification, taking both a positive and a negative unit value for $\Delta V_{tx,t}$ (this modelling decision accounts for the two voltage groupings seen in Fig. 1). In this way, the optimization tool derives settings that are suitable for every load and generation combination, considering both the highest and the lowest transmission system voltage that can the network sustain exposure to without resuming conventional transformer tapping.

The formulation of (1) implicitly motivates a large setting for *S*, as greater voltage deviations tend to invoke greater corrective reactive power flows. This formulation exploits some of the problem's inherent characteristics, so the optimization operates to *maximize* the network's reactive power responsiveness (the horizontal scale in Fig. 1), while also *defining* and *maximizing* the permissible transmission-side voltage range over which this response is feasible (the vertical scale in Fig. 1). Note that *S* is unbounded within the optimization, as its extent is implicitly bounded by the voltage limits that are enforced within the network.

4) Generator Voltage Controller Implementation

Under the autonomous control scheme, each distributed generator regulates the voltage at its connection point. This is modelled uses a droop slope, where the prevailing reactive power operating point acts as linear bias on the connection point target voltage. This archetypal scheme [25] promotes smoother co-operation between adjacent voltage controllers, and its merits for wind farms have been demonstrated [26].

As the optimization methodology is predicated on a steady-state power flow model, imposing a constraint on generator reactive power output relative to the prevailing connection point voltage gives an equilibrium operating point that each controller may realise.

A sigmoidal approximation of the bounded-linear relationship implied by droop control is employed [27], as illustrated in Fig. 2. This avoids the discontinuities encountered on reaching machine capability limits, which are problematic when a piece-wise linear description is used. The mathematical realization on the relationship shown in Fig. 2 is presented at more length in the Appendix (A) Note that Fig. 2 shows $q_{g,t}$ limiting on reaching the bounds of the prevailing capability range, $q_{g,t,range}$ (see, e.g, Appendix Fig. 11)

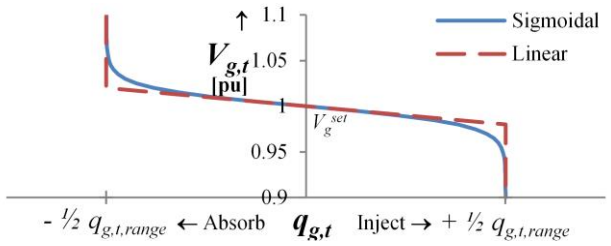

Fig. 2 Example relationship between the voltage at the generator interconnection point, $V_{g,t}$, and the reactive power regime invoked, $q_{g,t}$.

An innovative feature of the optimization tool is that generator voltage set points, V_g^{set}, and droop percentages V_g^{droop}, are both treated as control variables; the tight voltage limits on distribution systems suggest explicit optimization of each.

5) Generator Reactive Power Capability

The active power output of each generator for each scenario is an input parameter in the optimization framework. As such, the corresponding range of reactive power capability, defined by any arbitrary generator capability chart, is also an input parameter, denoted q_g^{range}, bounding the voltage control regime depicted in Fig. 2.

B. Optimal Power Flow for Smart Control

The use of optimal power flow techniques to centrally dispatch reactive power from distributed generators is well represented in the literature [28-30] In the present example, the entire power system is modelled holistically, embracing both the distribution and transmission systems.

1) Time Series Analysis

The multi-scenario approach can be dispensed with here, instead each period is considered independently. The optimization tool is invoked sequentially, with generation and load levels updated in each period.

2) Smart Objective Function

The objective function in this case is quite intuitive: the minimization of the deviation of the voltage at each of the controlled buses in the transmission system, $V_{tx,}^{c}$, taking the square to ensure a positive value:

$$min \quad \sum_{V_{tx}^{c}} (V_{tx}^{c} - V_{tx}^{set})^2 \quad (3)$$

3) Smart Control Variables

Under this scheme, the reactive power dispatch of each distributed generator, q_g, is simply a free variable, appropriately bounded within its machine limits:

$$-\tfrac{1}{2} q_{g,range} < q_g < \tfrac{1}{2} q_{g,range} \quad (4)$$

The tap setting of each bulk supply transformer is treated in a similar fashion:

$$T_{BSP}^{Ratio-} < T_{BSP}^{Ratio} < T_{BSP}^{Ratio+} \quad (5)$$

III. Test Platform

A. Test Networks

The well-known IEEE 30 bus test system recommends itself as suitable for the present work. It includes both transmission (132 kV) and distribution (33 kV) voltage levels, and serves a max load of 281 MW (see system parameters in [19], and in the Appendix).

1) Test Network Modifications

One notable modification is made to the test system, and with some justification: the sectionalisation of the meshed 33kV network to give three distinct distribution networks, *DxA*, *DxB* & *DxC*, each independently interfacing with the transmission system via its own bulk supply transformer, as shown in Fig. 3. Without such sectionalisation, achieved here by removing the branches linking buses *23-24*, *18-19*, *16-17* and *24-25*, transmission system power flows may wheel through the distribution system, an irregular state of affairs which does not align with standard industry practice.

A number of other alterations were also made to the test system. Most importantly, eight distributed generators, totalling 116MW, were connected at various arbitrary buses in the distribution networks. Also, to make clear the transmission/distribution system boundary that is important to this work, the three-winding transformers were replaced by two-winding equivalents, with the affected synchronous machines connecting directly to the adjacent transmission system bus. In this way, the transformers coupling the 132 kV system to the 33 kV networks function solely as bulk supply transformers, and do not fulfil a secondary role as a generator unit-transformer.

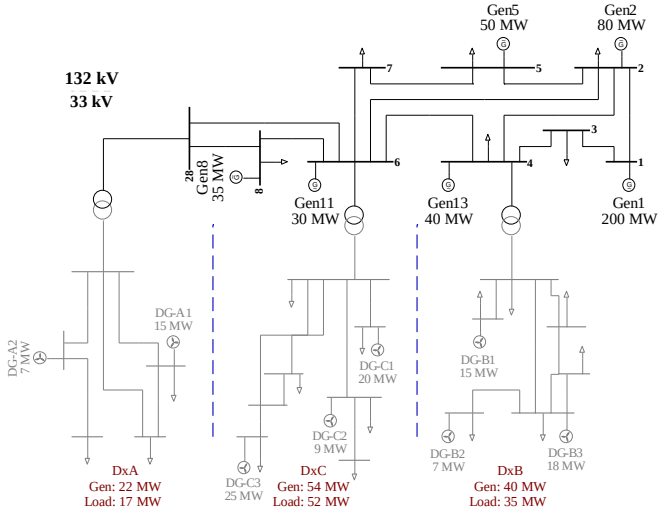

Fig. 3 Single line diagram for the modified IEEE 30 bus system, showing the sectionalisation of the 33 kV system into networks *DxA*, *DxC* and *DxB*.

2) Time Series Data

The Irish system load curve at fifteen minute granularity for the year 2011 [31] was used to scale each load in the test system, adding 5% Gaussian noise to provide some diversity, while not exceeding spot load maxima. Corresponding export data for eight Irish wind farms of appropriate size and proximity supplied output profiles for the eight distributed generators. A deterministic unit commitment and dispatch to serve the remaining net load was performed using the tool described in [32], based on generator cost characteristics given in [33]. This realistic generator dispatch has an important effect on transmission system power flows and voltages, and so undergirds all results presented.

The aggregate load and generation time series data for each distribution network was binned to a 10% granularity for use within the optimization tool to derive the autonomous settings, following an equivalent process to [16]. This gave around 80 representatives scenarios for each network, each of which being duplicated for high and low external voltage conditions.

The desired threshold voltage for each network, V_{thresh}, was selected based on load-flow studies of the holistic test system, by taking the median voltage at each bulk supply bus, assuming zero reactive power exchange with the voltage-responsive distribution networks. This provided a loose estimate, adequate for demonstration purposes, of the typical voltage range each distribution network might be exposed to.

B. Software Environment

The optimization tool was formulated within the AIMMS [34] environment, employing the reduced-gradient CONOPT 3.14V [35] solver. Validation load flow simulations were performed using DigSilent PowerFactory [36].

IV. Optimization Results

A. Autonomous Control Optimization Performance

The level of voltage-responsive performance available autonomously from each distribution network varied markedly, as shown in Table II. For each network, the two aspects of the objective function are decomposed, showing the average reactive power exchange, q_{tx}, realized for both the over- and under- voltage periods, in addition to the maximum and minimum values of V_{tx} that can be withstood. The variance in performance available appears closely linked to the loading on each network: *DxA*, with the lowest loading, achieves a high value for *S* and good average q_{tx} behaviour, *DxB* is in the middle in both respects, while *DxC* is heavily loaded and cannot achieve meaningful autonomous performance.

TABLE I: Autonomous Generator Settings

Generator	Network	Set Point (kV)	Droop
DG-A1	*DxA*	34.41	1%
DG-A2	*DxA*	34.06	1%
DG-B1	*DxB*	34.64	1%
DG-B2	*DxB*	34.61	1%
DC-B3	*DxB*	34.55	1%

TABLE II: Autonomous Network Performance

Network	Max V_{tx} (kV)	Min V_{tx} (kV)	Avg $q_{tx} \mid V_{tx} > V_{thresh}$ (MVAr)	Avg $q_{tx} \mid V_{tx} < V_{thresh}$ (MVAr)
DxA	*140.56*	134.21	-4.00	2.41
DxB	*141.83*	136.30	-7.92	0.49
DxC	*140.0*	139.5	-9.12	-8.22

1) DxA Autonomous Settings

This network can autonomously operate at a fixed transformer ratio of 4.033, corresponding to tap number 1, over the range of 6.35 kV implied by *S*, using generator settings as given in Table I. The droop setting of 1% is at the arbitrary lower bound imposed within the optimization.

TABLE III: *DxA* BINDING SCENARIOS

Scenario			Binding Condition
V_{tx} *(kV)*	*Load (%)*	*Gen (%)*	
140.56	30	0	Bus 27 at upper limit
134.21	100	0	Bus 30 at lower limit

The network's internal voltage limits, of ±5% around the nominal, are a key driver of the performance available. Voltage-driven limitations in just two of the scenarios considered, described in Table III, are the principal restraint on the magnitude of the crucial scaling variable, *S*. These binding scenarios accord with intuition: the minimum loading scenario, of 30%, suggests minimal voltage drop within the network, and so an increase in V_{tx}, above 140.56 kV, would bring bus 27 over its upper limit when the tap-changer is blocked. Conversely, the 100% loading scenario will see substantial internal voltage drop, and so *S* is selected to prevent the exposure of the network to external voltages below 134.21 kV.

2) DxB Autonomous Settings

Using the generator settings given in Table I, and at tap number 1, near the optimal ratio of 4.047, the *DxB* network can operate over the range of 5.53 kV implied by *S*. Internal upper voltage limits become binding in four of the considered scenarios for *DxB*, at three separate buses, with the lower voltage limit becoming binding at just one bus for one scenario, as displayed in Table IV. The interplay of load, generation, and locational effects illustrates how potentially binding conditions cannot be readily identified using analytic techniques.

TABLE IV: *DxB* BINDING SCENARIOS

Scenario			Binding Condition
V_{tx} *(kV)*	*Load (%)*	*Gen (%)*	
141.82	30	0	Bus 12 at upper limit
141.82	40	10	Bus 12 at upper limit
141.82	30	50	Bus 16 at upper limit
141.82	40	90	Bus 18 at upper limit
136.30	100	0	Bus 23 at lower limit

3) DxC Autonomous Settings

The results for the *DxC* network are underwhelming, as shown in Table II. In essence, the network's electrical characteristics, and the magnitude of the connected loads, precludes the blocking of transformer tapping over any meaningful range of transmission system voltages. Even with a fixed external voltage, 95.8% of the permissible range of internal voltages is exploited, corresponding to the load-driven voltage drop in the full load, zero generation scenario. Here, 1.29 kV is dropped between bus 10 and the remote bus 24, in addition to 1.87 kV dropped internal to the bulk supply transformer, with the network serving a load of 52 MW and 29.8 MVAr. A lower external voltage here would breach the lower voltage limit for this high load scenario, and raising it would breach the upper limit in low load conditions. Fundamentally, the power flows the network is exposed to, and the impedance of its conductors, means that uninterrupted tap-changing action is indispensable to maintain an acceptable internal voltage profile: this illustrates the importance of distribution system characteristics in determining the aggregate reactive power resource capability. The generators in *DxC* are operated in unity mode in subsequent validations, except in the *smart* case.

B. Smart Control Optimization Performance

The *smart* optimization performance was encouraging, converging to a locally optimal solution for the global system in 99.8% of the time series points considered over the test year. The resulting system behaviour is best discussed in the following section, alongside the equivalent, externally validated time series results for the *autonomous* control.

V. SIMULATION RESULTS

For each control scheme a load flow analysis of the holistic power system was performed every fifteen minutes. For *autonomous* control, the voltage control settings derived from the optimization methodology were implemented, and tap-blocking was maintained unless a calculation returned a high-side voltage outside of the permissible range, in which case normal tap-changing was enabled. For the *smart* control scheme, the reactive power set points and tap positions were taken directly from the optimization results for the corresponding period. Two other control strategies were also simulated: a simple *unity* case, where distributed generators make no reactive power contribution, and a *simplistic* voltage control case, where voltage control is enabled for distributed generators, at notional set-points of 33.83 kV at 1% droop, and with bulk supply transformers operating as typical to regulate the low-side voltage to 33 kV ± 1%.

1) Voltage Response Discussion

The central themes of this paper are embodied graphically in Figs. 4 – 9. These figures compare how the networks actually responded to their organically fluctuating external voltages, which varied over a broad range as dictated by loading and dispatch conditions. These figures plot the voltage and reactive power exchange level recorded at each network's bulk supply bus for each fifteen minute period within the simulation. The following treatment will draw out some of the figures' salient features, directing the eye to the noteworthy comparisons. Throughout, points plotted in the darker tone denote those periods where local generation levels exceeded 20% of capacity, indicating the availability of a reactive power resource (see Fig. 11).

The central results of this paper are given in Fig. 6 and Fig. 7, which shows the actual performance of the *autonomous* settings. The desired behaviour is clearly evident in periods where wind generation levels are non-negligible. The networks respond in an appropriately linear fashion to voltage fluctuations at the transmission node, injecting reactive power

as the voltage magnitude declines, and absorbing when it rises. Furthermore, the voltage-responsive reactive power flows compress the range of voltages arising at the transmission connection bus, bringing most within the feasible range shown by the dashed lines, within which the network can dispense with tap-changer functionality. This harmonious interplay can be summarized in an aphorism: *voltage responsive distribution networks make transmission system voltages more consistent, making tap changers less necessary, allowing distribution networks to be more voltage responsive*.

An interesting feature is depicted in Fig. 7, where the maximum export of reactive power achieved is only ~2.5 MVAr. The selection of the crucial V_{thresh} seems to account for this rather modest value. Without depressed external voltages, the network isn't driven to export reactive power, and this explains the preponderance of absorption in Fig. 7. Visual inspection suggests that extrapolating the voltage response characteristic downwards would see it intersect with the dashed lower voltage marker at around 5 MVAr.

The difference in the disposition of the darker operating points between, for instance, Fig. 4 and Fig. 6 makes a strong argument against the *simplistic* control regime. The implied slope in Fig. 4 is alarming: lower transmission system voltages are here associated with a greater absorption of reactive power. This undesirable relationship can largely be explained by unhelpful tap-changer action: note the striations evident in the dark cloud of operating points to the right of the figure. Here, each striation corresponds to a discrete tap setting, and each of these is, in itself, appropriately sloped. However, the cumulative effect of stepping between taps gives an aggregate response that loses, and inverts, the desired relationship.

Finally, the performance of the *smart* control scheme is shown in Fig. 8 and Fig. 9. It is clear that in many periods the connection point voltage is brought to precisely the desired value, dispensing with the regulation slope enforced by the *autonomous* scheme. Also notable is that even with an optimal dispatch of reactive power, in many periods the requisite resource is not available, and the transmission-side voltage cannot be effectively regulated.

2) Reactive Power Exchange Discussion

The histograms presented in Fig. 10 reward careful study, showing how three distinct control schemes affect the reactive power behaviour of each distribution network over the test year. Consider first the *unity* cases, not previously discussed. These histograms depict the natural reactive power behaviour of each network. The trend is clear: *DxA* consumes modest levels of reactive power, *DxB* a little more, and *DxC* considerable amounts. Voltage-responsive behaviour implies a reactive power histogram balanced about the vertical axis, sometimes injecting and sometimes absorbing, as dictated by voltage conditions. From the *unity* cases, each network needs a greater-or-lesser rightward shift in Fig. 10 to achieve this. This shift is given to a degree under the *autonomous* control, most successfully for the *DxA* network. *Smart* control gives a further slight shift right, however it is notable that even with this, *DxC* can only inject reactive power in the rarest of circumstances.

The special value of the *smart* control is illustrated by the shape of its reactive power histograms. For *DxA* and *DxB*, clear peaks are in evidence on either side of the vertical axis. This is because the *smart* scheme can explicitly dispatch each network to these injection and absorption limits over many periods, while the *autonomous* scheme must rely on comparatively rare external voltage conditions to invoke this type of response. Notably, *DxC* cannot deliver this style of response.

3) Broader Performance Metrics

a) Distribution System Voltage Performance

Under *autonomous* control, within the *DxA* network, internal voltages ranged from 31.61 kV to 34.64 kV, fully exploiting the range available without causing any breaches. In *DxB*, the range was 31.76 kV to 34.70 kV: these slight over-voltages manifested in less than 0.8% of the year, being a consequence of the quantization of the optimal transformer ratio to the nearest discrete tap.

b) Transmission System Voltage Performance

The *autonomous* utilization of the embedded reactive resources had a modest, yet positive, impact on global transmission system performance, as shown in Table V. In interpreting the results it must be borne in mind that the two relevant networks, *DxA* and *DxB*, between them only accommodated 18.34% of the system's annual demand, and their generation supplied 7.73% of the system's energy. Compared with *unity* operation, *autonomous* operation had a compressive effect on system voltages, reducing standard deviations both at the relevant bulk supply buses and across the wider transmission system, with these effects particularly pronounced when wind outputs exceeded 20% of installed capacity. By contrast, the *smart* scheme acted to increase transmission voltages, while tending to also increase standard deviation.

VI. Conclusions

It has been demonstrated that optimally-selected voltage control settings for distributed generators, coupled with repurposed tap-blocking functionality, can autonomously deliver voltage-responsive reactive power flows to the transmission system. A greater voltage responsive behaviour is achieved using centrally dispatched smart grid scheme, however such schemes cannot fully overcome the network limitations that may impede the export of reactive power from distribution systems. Notably, the smart control scheme can drive the distribution networks to their reactive power limits in many periods to enforce as much voltage-controlling effect as possible, whereas the autonomous control delivers a gentler response, maintaining voltages within a range rather than enforcing a precise setpoint.

Fundamentally, it is challenging to deliver reactive power from distributed resources to the transmission system. Innovative, or elaborate, control schemes can overcome such challenges to varying degrees, however the test results presented in this paper suggest that only modest effects on the transmission system voltage profile can be anticipated.

DxA Simplistic Voltage Response

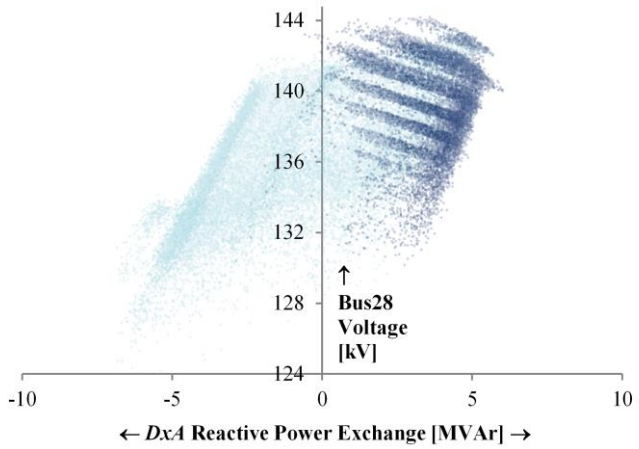

Fig. 4 The voltage responsive performance achieved by the *DxA* network, without optimized voltage control settings or special treatment of the bulk supply transformer.

DxB Simplistic Voltage Response

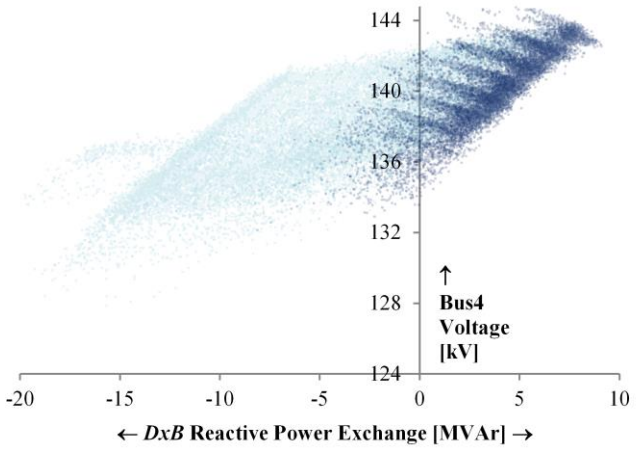

Fig. 5 The voltage responsive performance achieved by the *DxB* network, without optimized voltage control settings or special treatment of the bulk supply transformer.

DxA Autonomous Voltage Response

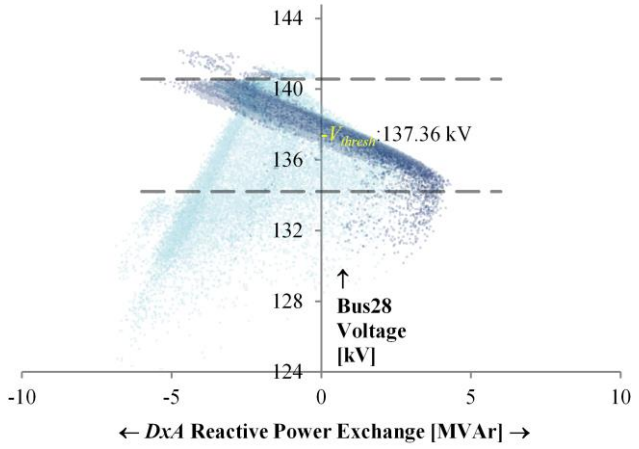

Fig. 6 The voltage responsive performance achieved by the *DxA* network, where the dashed lines indicate the voltage range over which the network can operate at its optimally selected static tap setting.

DxB Autonomous Voltage Response

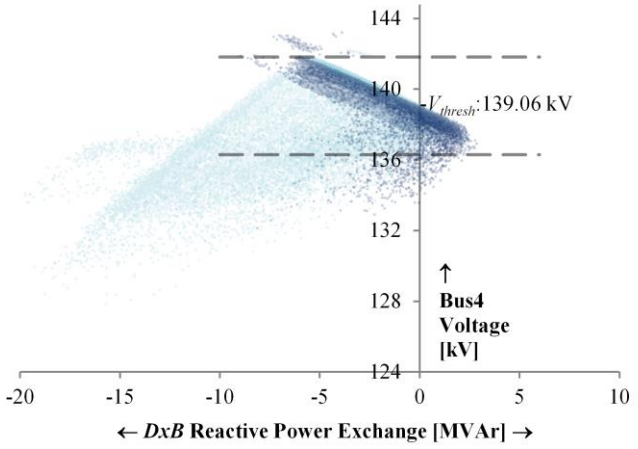

Fig. 7 The voltage responsive performance achieved by the *DxB* network, where the dashed lines indicate the voltage range over which the network can operate at its optimally selected static tap setting.

DxA Smart Voltage Response

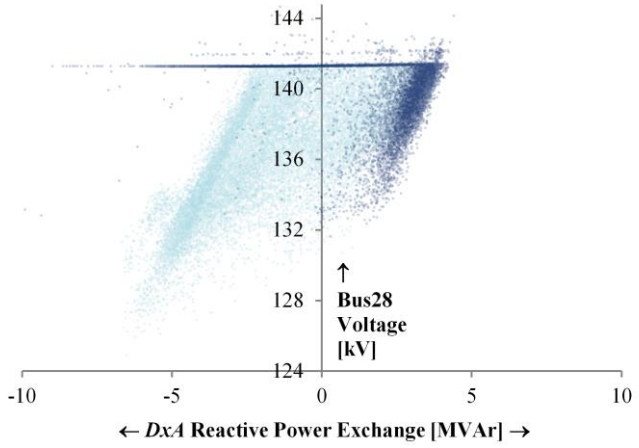

Fig. 8 The voltage responsive performance achieved by the *DxA* network, where tap positions and reactive power operating points are optimally dispatched from period to period

DxB Smart Voltage Response

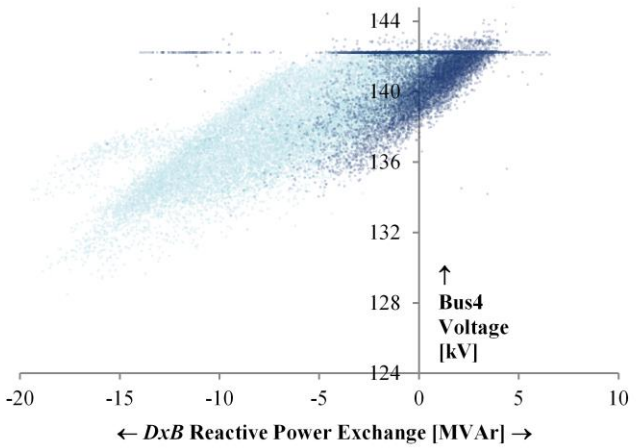

Fig. 9 The voltage responsive performance achieved by the *DxB* network, where tap positions and reactive power operating points are optimally dispatched from period to period

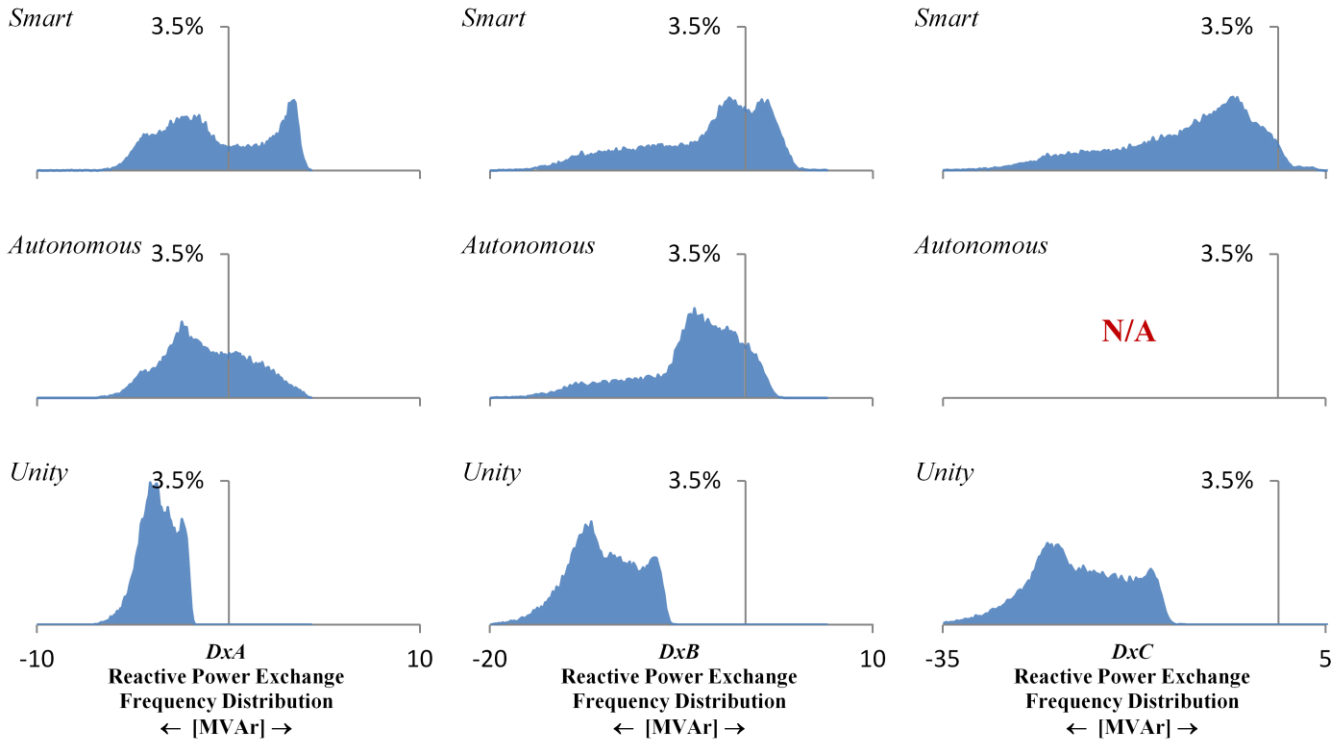

Fig. 10 The frequency distribution of the reactive power exchange level for each network under three progressively more advanced control schemes

TABLE V : TRANSMISSION SYSTEM VOLTAGE METRICS

	Entire Test Year		Wind > 20% Capacity	
	Median Volt. (kV)	**Volt. Std. Dev. (kV)**	**Median Volt. (kV)**	**Volt. Std. Dev. (kV)**
Bus4				
Unity	137.39	2.46	138.01	2.07
Simplistic	139.23	2.74	140.36	1.98
Autonomous	138.83	2.24	139.39	1.36
Smart	140.25	2.63	141.78	1.47
Bus28				
Unity	135.60	3.02	136.46	2.53
Simplistic	137.70	3.33	139.14	2.37
Autonomous	137.18	2.73	137.94	1.66
Smart	139.02	3.17	141.03	1.67
All Transmission Buses				
Unity	138.22	3.65	138.99	2.88
Simplistic	139.65	3.49	141.01	2.41
Autonomous	139.06	3.31	139.72	2.36
Smart	140.56	3.25	141.44	1.82

APPENDIX

A. Sigmoidal Voltage Control Implementation

The relationship shown in Fig. 2 is enforced by the following equality constraint:

$$q_{g,t} = \left[\left(\frac{1}{1+e^{\alpha_{g,t}(V_{g,t}-V_g^{set})}}\right)-0.5\right]q_{g,t,range} \quad (6)$$

To select the shaping variable, $\alpha_{g,t}$, of the sigmoid function appropriately, we note the derivative at the y-axis crossing in Fig. 2:

$$\left.\frac{dV_{g,t}}{dq_{g,t}}\right|_{q_{g,t}=0} = \frac{4}{q_{g,t,range}\alpha_{g,t}} \quad (7)$$

Accordingly, the following equality constraint defines the appropriate value of $\alpha_{g,t}$ to ensure a voltage-regulation slope congruent with the droop percentage, V_g^{droop}, acknowledging the varying extent of $q_{g,t,range}$, and the rated reactive power of the generator, $q_{g,rated}$.

$$\alpha_{g,t} = \frac{4q_{g,rated}}{-q_{g,t,range}\left(V_g^{set}V_g^{droop}\right)} \quad (8)$$

B. Test System Details

Conventional generators are modelled with a capability chart per [37], and regulate their terminal voltage to 145.2 kV when online, with a droop of 4% on a rated reactive power of 0.5 pu.

TABLE VI : TRANSFORMER DATA

Transformer	Sht. Cct. Volt	S_{rated} (MVA)	Volt per tap	Tap positions
4-12	25.6 %	100	1 %	± 10
6-10	16.8 %	100	1 %	± 10
28-27	39.6 %	100	1 %	± 10

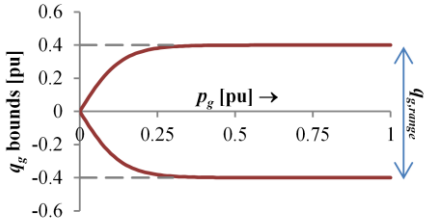

Fig. 11 Reactive power capability chart for the distributed generators

REFERENCES

[1] J. O'Sullivan, Y. Coughlan, S. Rourke, and N. Kamaluddin, "Achieving the Highest Levels of Wind Integration: A System Operator Perspective," *Sustainable Energy, IEEE Transactions on*, vol. 3, 2012.

[2] "Facilitiation of Renewables Wp3 Final Report," EirGrid Plc.June 2010.

[3] X. Le, *et al.*, "Wind Integration in Power Systems: Operational Challenges and Possible Solutions," *Proceedings of the IEEE*, vol. 99, 2011.

[4] A. C. Rueda-Medina and A. Padilha-Feltrin, "Distributed Generators as Providers of Reactive Power Support - a Market Approach," *Power Systems, IEEE Transactions on*, vol. 28, 2013.

[5] V. Akhmatov and P. B. Eriksen, "A Large Wind Power System in Almost Island Operation - a Danish Case Study," *Power Systems, IEEE Transactions on*, vol. 22, 2007.

[6] S. Engelhardt, I. Erlich, C. Feltes, J. Kretschmann, and F. Shewarega, "Reactive Power Capability of Wind Turbines Based on Doubly Fed Induction Generators," *Energy Conversion, IEEE Transactions on*, vol. 26, 2011.

[7] P. Cuffe, E. Lannoye, A. Keane, and A. Tuohy, "Unit Commitment Considering Regional Synchronous Reactive Power Requirements: Costs and Effects," presented at the 11th Wind Integration Workshop, Lisbon, Portugal, 2012.

[8] F. B. Alhasawi and J. V. Milanovic, "Techno-Economic Contribution of Facts Devices to the Operation of Power Systems with High Level of Wind Power Integration," *Power Systems, IEEE Transactions on*, vol. 27, 2012.

[9] C. Hsiao-Dong, *et al.*, "Effect of Voltage Stability Constraints and Corrective Control on Pricing Components," in *Power and Energy Society General Meeting - Conversion and Delivery of Electrical Energy in the 21st Century, 2008 IEEE*, 2008.

[10] Z. H. Rather, Z. Chen, and P. Thogersen, "Challenges of Danish Power System and Their Possible Solutions," in *Power System Technology (POWERCON), 2012 IEEE International Conference on*, 2012.

[11] T. Sansawatt, L. F. Ochoa, and G. P. Harrison, "Integrating Distributed Generation Using Decentralised Voltage Regulation," in *Power and Energy Society General Meeting, 2010 IEEE*, 2010.

[12] T. Sansawatt, L. F. Ochoa, and G. P. Harrison, "Smart Decentralized Control of Dg for Voltage and Thermal Constraint Management," *Power Systems, IEEE Transactions on*, vol. 27, 2012.

[13] P. Cuffe, P. Smith, and A. Keane, "Characterisation of the Reactive Power Capability of Diverse Distributed Generators: Toward an Optimisation Approach," in *IEEE Power and Energy Society General Meeting*, San Diego, CA, USA, 2012.

[14] P. Cuffe, P. Smith, and A. Keane, "Capability Chart for Distributed Reactive Power Resources," *Power Systems, IEEE Transactions on*, vol. 29, 2014.

[15] P. Cuffe, P. Smith, and A. Keane, "Effect of Energy Harvesting Network Reactive Support on Transmission System Voltage Performance," presented at the 21st International Conference on Electricity Distribution, Frankfurt, 2011.

[16] L. F. Ochoa, A. Keane, and G. P. Harrison, "Minimizing the Reactive Support for Distributed Generation: Enhanced Passive Operation and Smart Distribution Networks," *Power Systems, IEEE Transactions on*, vol. 26, 2011.

[17] M. Džamarija, M. Bakhtvar, and A. Keane, "Operational Characteristics of Non-Firm Wind Generation in Distribution Networks," in *IEEE Power and Energy Society General Meeting*, San Diego, CA, USA, 2012.

[18] P. Cuffe, P. Smith, and A. Keane, "Capability Chart for Distributed Reactive Power Resources," *Power Systems, IEEE Transactions on (early access)*, 2013.

[19] O. Alsac and B. Stott, "Optimal Load Flow with Steady-State Security," *Power Apparatus and Systems, IEEE Transactions on*, vol. PAS-93, 1974.

[20] C. J. Dent, L. F. Ochoa, G. P. Harrison, and J. W. Bialek, "Efficient Secure Ac Opf for Network Generation Capacity Assessment," *Power Systems, IEEE Transactions on*, vol. 25, 2010.

[21] L. F. Ochoa, C. J. Dent, and G. P. Harrison, "Distribution Network Capacity Assessment: Variable Dg and Active Networks," *Power Systems, IEEE Transactions on*, vol. 25, 2010.

[22] L. G. Meegahapola, S. R. Abbott, D. J. Morrow, T. Littler, and D. Flynn, "Optimal Allocation of Distributed Reactive Power Resources under Network Constraints for System Loss Minimization," in *Power and Energy Society General Meeting, 2011 IEEE*, 2011.

[23] L. F. Ochoa and G. P. Harrison, "Using Ac Optimal Power Flow for Dg Planning and Optimisation," in *Power and Energy Society General Meeting, 2010 IEEE*, 2010.

[24] C. D. Vournas and G. A. Manos, "Emergency Tap-Blocking to Prevent Voltage Collapse," in *Power Tech Proceedings, 2001 IEEE Porto*, 2001.

[25] J. D. Hurley, L. N. Bize, and C. R. Mummert, "The Adverse Effects of Excitation System Var and Power Factor Controllers," *Energy Conversion, IEEE Transactions on*, vol. 14, 1999.

[26] N. Miller, *et al.*, "Coordinated Voltage Control for Multiple Wind Plants in Eastern Wyoming: Analysis, Field Experience and Validation," presented at the 11th Wind Integration Workshop, Lisbon, Portugal, 2012.

[27] P. N. Vovos, A. E. Kiprakis, A. R. Wallace, and G. P. Harrison, "Centralized and Distributed Voltage Control: Impact on Distributed Generation Penetration," *Power Systems, IEEE Transactions on*, vol. 22, 2007.

[28] F. A. Viawan and D. Karlsson, "Coordinated Voltage and Reactive Power Control in the Presence of Distributed Generation," in *Power and Energy Society General Meeting - Conversion and Delivery of Electrical Energy in the 21st Century, 2008 IEEE*, 2008.

[29] M. Oshiro, *et al.*, "Optimal Voltage Control in Distribution Systems Using Pv Generators," *International Journal of Electrical Power & Energy Systems*, vol. 33, 2011.

[30] Y. Chistyakov, E. Kholodova, K. Netreba, A. Szabo, and M. Metzger, "Combined Central and Local Control of Reactive Power in Electrical Grids with Distributed Generation," in *Energy Conference and Exhibition (ENERGYCON), 2012 IEEE International*, 2012.

[31] EirGrid. "System Demand" [Online]. Available: http://www.eirgrid.com

[32] A. Shortt, J. Kiviluoma, and M. O'Malley, "Accommodating Variability in Generation Planning," *Power Systems, IEEE Transactions on*, vol. 28, 2013.

[33] I. J. Raglend and N. P. Padhy, "Solutions to Practical Unit Commitment Problems with Operational, Power Flow and Environmental Constraints," in *Power Engineering Society General Meeting, 2006. IEEE*, 2006.

[34] M. Roelofs and J. Bisschop, *Aimms - the User's Guide.*: Paragon Decision Technology, 2011.

[35] A. S. Drud, "Conopt—a Large-Scale Grg Code," *ORSA Journal on Computing*, vol. 6, 1994.

[36] D. P. F. Manual and D. PowerFactory, "Version 14.0," *DIgSILENT GmbH, Gomaringen, Germany*, 2009.

[37] P. Cuffe, P. Smith, and A. Keane, "Transmission System Impact of Wind Energy Harvesting Networks," *Sustainable Energy, IEEE Transactions on* 2012 *doi:* 10.1109/tste.2012.2199342.

Paul Cuffe received B.E. and Ph.D. degrees in Electrical Engineering from University College Dublin in 2009 and 2012, respectively. He is currently a senior researcher within the Electricity Research Centre, University College Dublin (UCD), Ireland. His research interests are in reactive power management, distribution generation and power system visualization techniques.

Andrew Keane received B.E. and Ph.D. degrees in Electrical Engineering from University College Dublin in 2003 and 2007 respectively. He is a lecturer with the School of Electrical, Electronic and Communications Engineering, UCD, Ireland, with research interests in power systems planning and operation, distributed energy resources and distribution networks.